

Article

Insights into Della Robbia's Terracotta Monument to Cardinal Federighi: Raw Materials and Technologies

Donata Magrini ^{1,*} , Emma Cantisani ¹, Silvia Vettori ¹ and Kaare Lund Rasmussen ²

¹ CNR-ISPC, National Research Council—Institute of Heritage Science, Via Madonna del Piano 10, 50019 Florence, Italy; emma.cantisani@cnr.it (E.C.); silvia.vettori@cnr.it (S.V.)

² CHART, Cultural Heritage and Archaeometric Research Team, Department of Physics, Chemistry and Pharmacy, University of Southern Denmark SDU, Campusvej 55, 5230 Odense, Denmark; klr@sdu.dk

* Correspondence: donata.magrini@cnr.it

Abstract: The present work comprises the application of a multi-analytical strategy based on the combination of several non-destructive and micro-invasive methodologies for the examination of the glazed tiles from the tomb of Benozzo Federighi made by Luca della Robbia. The marble tomb is framed by flat glazed terracotta tiles, each ornamented with naturalistically depicted flowers. The tiles are assembled like an “opus sectile” and their background is gilded. The leaf is incorporated on the top of the glaze, differently by traditional gilding technique as in previous glazed works of della Robbia. The identification methodology integrates the results from spot analyses such as UV-vis reflectance spectroscopy and X-ray fluorescence, with those obtained on tiny samples by X-ray diffraction, electron microscopic observations, laser ablation inductively coupled plasma mass spectrometry and firing temperature analysis. The adopted analytical protocol allowed us to clarify peculiarities of the artist's technique and of the manufacturing technology used to create the terracotta and gilded glazed tiles. The terracotta body shows main phases related with Ca-rich ceramic body and the glaze results Pb-based and additioned with Sn as an opacifier. Co, Pb-Sb and Cu were identified as glazes colouring agents. The hypothesis on the use of the “third firing” technique for gilding tiles is explored in the text.

Keywords: Luca della Robbia; glazed terracotta; gilding technique; multi-analytical approach; chemical elemental analyses; compositional studies; firing temperature



Citation: Magrini, D.; Cantisani, E.; Vettori, S.; Rasmussen, K.L. Insights into Della Robbia's Terracotta Monument to Cardinal Federighi: Raw Materials and Technologies. *Appl. Sci.* **2022**, *12*, 4304. <https://doi.org/10.3390/app12094304>

Academic Editor: Alba Patrizia Santo

Received: 22 March 2022

Accepted: 22 April 2022

Published: 24 April 2022

Publisher's Note: MDPI stays neutral with regard to jurisdictional claims in published maps and institutional affiliations.



Copyright: © 2022 by the authors. Licensee MDPI, Basel, Switzerland. This article is an open access article distributed under the terms and conditions of the Creative Commons Attribution (CC BY) license (<https://creativecommons.org/licenses/by/4.0/>).

1. Introduction

The funeral monument of Benozzo Federighi, bishop of Fiesole, was created by Luca della Robbia (1399/1400–1482) in 1454 and was originally located in the church of San Pancrazio. The artwork is characterised by a floral frame made using glazed and gilded terracotta tiles with different shapes and bright colours, assembled like an “opus sectile”. The sculpture of Bishop Federighi is placed on top of an ancient-style sarcophagus, inserted into the wall, with two angels holding a laurel wreath inside which the name of the deceased is carved in Latin. At the bottom of the niche, the high relief figure of Christ is depicted with the Madonna and St. John on either side (Figure 1). A recent conservational project consisted of a delicate and balanced cleaning to recover and enhance the processing of the surfaces, and also highlighting the traces of gilding and polychromy on the marble.

The frame appears to have been made by engraving the raw unfired clay, then covered by a glaze in a second firing event. This effect was firstly noted by Gerspack [1]. He stated that each of the twenty-four ovals and four roundels which make up the frame, were in turn formed by small fragments all separated and joined together as in the mosaic technique. The incision made by Luca della Robbia, directly on the raw support, is particularly evident in certain areas where the support is not anymore covered by the gold, or by the glaze, or both. It is not a mosaic, but the effect is given by an engraving that highlights the golden

parts compared to the polychrome ones. The conjunction of the tiles is visible only in a few areas. It can, therefore, be hypothesized that the artist did not produce one tile at a time, but rather produced them as longer slabs. After having engraved them, he most likely cut them according to the outline of the design in hidden points. However, the most peculiar detail of this artwork remains the application of the golden foil. Starting from the conservators' indications, three main hypotheses can be suggested for its manufacture: (i) the use of cold-gilding technology; (ii) the presence of a "luster", a decorative metallic film applied on the surface of the glazed ceramics, obtained by a low-temperature (below 650 °C) controlled reduction of copper and silver compounds; (iii) what is called the "third firing" technique [1–4]. This latter technique has been used since ancient times, and it was applied above all to porcelain. The term "third firing" refers to the third firing event that is applied to an object or a tile that has already undergone two phases: (i) a first firing of the support; (ii) second firing of the glaze or glazing, to subsequently add the decorations in the multiple techniques. Already at the first step, the ceramic could be painted with the underglaze technique which guarantees a brilliant and unalterable result over time thanks to the subsequent vitrification. In the case of "third firing" process, the method of decorating is the overglazed technique. The powder colours or gold foil are blended with the addition of a fluid medium and are applied with a brush on the ceramic object. The latter is then subjected to a cooking of approximately 750–900°. During the firing, on-glaze materials melt with the vitreous coating of the ceramic, becoming one with it.



Figure 1. The Tomb of Bishop Benozzo Federighi by Luca della Robbia. Santa Trinita Church, Florence, Italy.

Numerous scholars have dealt with archaeometric analysis of the works of Luca della Robbia [5–14]. Many of these works were focused mainly on the characterization of glazes and raw materials such as the terracotta body, but no archaeometric study was previously performed on the artist's production, characterised by this experimental technique of gilding.

The Federighi monument has been studied in detail with regard to the historical value and as a piece of artwork [1,4,15,16], but no in-depth investigations have been made from an archaeometric point of view. In particular, as far as we know, there are currently no works dealing with this particular gilding technique. Normally, the golden decoration visible on other Luca della Robbia masterpieces, are manufactured by spreading the leaf gold with a binder, following the traditional "cold gilding" technique as in the "Altman Madonna" at the Metropolitan Museum, or in the "Virgin and Child" (called the Genoa Madonna) at the Detroit Institute of Arts.

Starting with these issues, the present study focuses first to examine and characterise the raw materials and the procedure to realise the glazed tiles, then to define the unique technique employed by della Robbia to decorate the golden tiles since as far as we know this technique is a unicum in the production of the artist.

2. Materials and Methods

The adopted protocol is based on a two-step survey. In the first part, non-destructive analyses were mainly performed in order to characterise the materials responsible for the colour of the tiles (Table 1) and to address the possibilities of micro-sampling. Micro-fragments (Figure 2 and Table 2) were collected to characterize the composition and the executive technique of gilding, glazes and terracotta bodies.

The description of the areas analysed by fibre optic reflectance spectroscopy (FORS), X-ray fluorescence (XRF) and documented by portable microscope are listed in Table 1.

Table 1. Areas analysed non-invasively by FORS and XRF and documented by portable microscope.

Sample's Name	Sample's Name
SX7_yellowdark1	SX4_white2
SX7_yellowlight1	SX4_white1
SX6_purple2	SX1_white1
SX6_purple1	SX1_lightblue1
SX6_graydark	BA3_olive1
SX6_graylight	BA1_blue1
SX6_yellow1	SX6_gilding6
SX5_greenmedium tone1	SX6_gilding5
SX5_yellow2	SX6_gilding4
SX5_yellow1	SX5_gilding3
SX4_greendark1	SX5_gilding2
SX4_greenmedium tone1	SX5_gilding1
SX4_greenlight1	DX6_gilding10
SX4_blue2	DX5_gilding9
SX4_blue1	DX5_gilding8
SX4_white3	DX4_gilding7

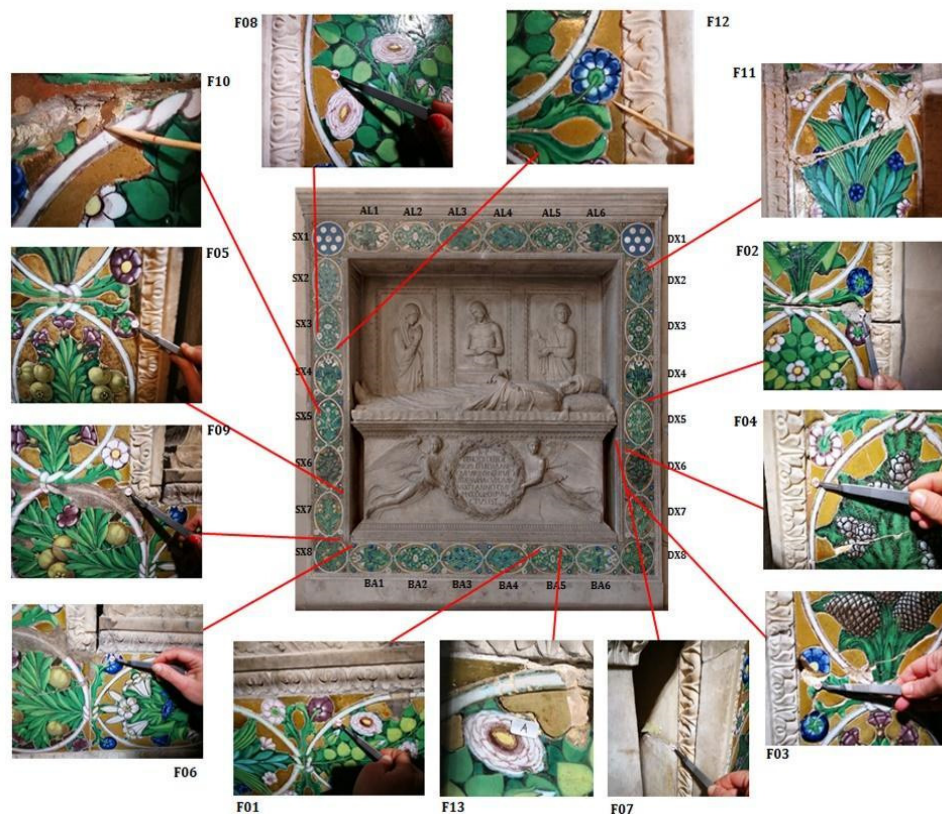


Figure 2. Location of the sampling areas and indication of the labels of the tile (AL, DX, BA, SX).

Table 2. Samples in the present study with the sample name, the numbering and the location on the Monument as shown in Figure 2 and the analytical techniques applied ¹.

Sample's Name	Sampling Description	Analytical Techniques Applied
F_01	Tile BA5. On an area with gilded glaze	OM, CS, SEM-EDS
F_02	Between DX4 and DX5. On the gilding.	OM, CS, SEM-EDS, XRPD
F_03	Tile DX6. Terracotta body	XRPD
F_04	Tile DX6 stucco sample	XRPD
F_05	Between SX6 and SX7 on the tile with darkened gilding	OM, CS, SEM-EDS, XRPD
F_06	Tile BA1. On the blue decoration where there are high copper signals. Stucco is also present	OM, CS, SEM-EDS
F_07	Brown adhesive on the back of a gilded tile.	OM
F_08	Powder from stucco	XRPD
F_09	Concrete	XRPD
F_10	Tile SX5. Pinkish stucco around the blue flower	XRPD
F_11	Fragment of terracotta and white plaster underneath	XRPD, LA-ICP-MS, firing temperature
F_12	Fragment of gilded terracotta tile	OM, CS, XRPD, SEM-EDS
F_13 a	Tile BA5. Fragment of terracotta	XRPD, LA-ICP-MS, firing temperature
F_13 b	Tile BA5. Fragment of terracotta	XRPD, LA-ICP-MS, firing temperature

¹ OM: Optical microscopy; CS: cross-section; SEM-EDS: electron microscope energy dispersive X-ray spectroscopy; XRPD: X-ray powder diffraction; ICP-MS: laser ablation-inductively-coupled Plasma mass spectrometry.

Fibre optic reflectance spectroscopy (FORS) in the UV-VIS range is a fast, non-destructive technique widely employed for colourant identification on glasses and glazes [17–22]. Spectra in the 350–900 nm range, were acquired by using a Tungsten source (Ocean Optics model HL200) and a spectrometer (Ocean Optics model HR2000) equipped with optical fibres. The measuring head with 45° illumination and 0° signal collection allowed the acquisition of the reflectance spectrum from an area of about 2 mm². Each acquired spectrum was the average of 30 scans. As a reference, a Spectralon© plate (WS-1S-L Labsphere

certified standard, 99% reflective material) was used. The acquired reflectance spectra were compared with reference spectra included in both ISPC-CNR spectral database (not published) and IFAC-CNR FORS spectral databases of pigments [23].

X-ray fluorescence (XRF) is a powerful technique for acquiring information about elemental composition of glazed terracotta [9,24–26]. XRF spectra were collected by a handheld Tracer III SD Bruker spectrometer, equipped with a rhodium anode and solid-state silicon detector with an energy dispersive detection system. The used set-up was: 40 kV acceleration, 12 μ A anode current and an acquisition time of 120 s. The measuring area was an elliptical spot of 4 \times 7 mm. For data treatment the ARTAX software was used after normalizing spectra to the intensity of Rh $K\alpha$ line at 20.21 keV.

As both FORS and XRF are non-destructive techniques, it was possible to acquire several spectra in different coloured areas for each tile, and also to repeat the measurements in some areas of the same colour on different spots. As far as physically possible, efforts have been made to perform the measurements on the same spot with the two techniques (XRF and FORS) also considering that the dimensions of the investigated areas are slightly different for the two methods.

A total of 32 spectra were acquired by both XRF and FORS. All the areas analysed were documented by a portable digital microscope with 25 \times magnification (Scalar DG-2A, optical zoom 25–200X, magnification @ 25X, field of view 13 \times 8 mm).

Guided by the results achieved during the non-destructive survey, 12 micro-samples plus a whole fragment of a tile with gilding (split in two and labelled FED_13a, b) were taken from the terracotta and from the gilded tiles, in order to perform micro-destructive analyses to help interpret data obtained by non-destructive analyses and characterise the stratigraphic sequence and the composition of the materials. The number of samples was limited to avoid further damage to the monument due to its great historical value. Among the listed samples, five were devoted to reconstructing the stratigraphic sequence and obtaining information about the manufacturing technology of the gilded tiles.

In Figure 2 is shown the image of the Federighi Monument with an indication of the sampling areas and the labels used to identify the tiles, listed in Table 2 along with the sample description and the applied analytical techniques.

X-ray powder diffraction (XRPD) was employed using a Philips X'Pert PRO in order to determine the mineralogical composition. A copper anticathode ($\lambda = 1.54 \text{ \AA}$) was used with the following settings: current 30 mA, acceleration voltage 40 kV, explored 2θ range between 3 and 70 $^\circ$, step size 0.02 $^\circ$ and stepping time 50 s. The XRPD analyses were performed on the terracotta samples and on the mortars.

Morphological and semi-quantitative microchemical analyses were obtained by means of a scanning electron microscopy with energy dispersive X-ray spectroscopy (SEM/EDS) ZEISS EVO MA 15 with a W-filament equipped with an analytical energy dispersion system from EDS/SDD, Oxford Ultimex 40 (40 mm 2 with a resolution of 127 eV @ 5.9 keV) and using the Aztec 5.0 SP1 software. The SEM/EDS measurements were performed on carbon coated cross sections of the samples with the following operative conditions: an acceleration voltage of 15 kV, 500 pA beam current, working distance between 9 and 8.5 mm; 20 s live time at an acquisition rate of at least 600.000 ct s $^{-1}$ on a Co-standard, processing time 4 for point analyses; 500 μ s pixel dwell time for maps acquisition with 1024 \times 768 pixels resolution.

The software used for the microanalysis was an Aztec 5.0 SP1 software that employs the XPP matrix correction scheme developed by Pouchou and Pichoir in 1991 [27]. This is a Phi-Rho-Z approach which uses exponentials to describe the shape of the $\phi(\rho z)$ curve. XPP matrix correction was chosen because of its favourable performance in situations of severe absorption such as the analysis of light elements in a heavy element matrix. The procedure is a “standard-less” quantitative analysis that employs pre-acquired standard materials for calculations. The monitoring of constant analytical conditions (i.e., filament emission) is archived with repeated analyses of a Co metallic standard.

LA-ICP-MS was performed using a CETAC LXS-213 G2 equipped with a NdYAG laser operating at the fifth harmonic at a wavelength of 213 nm. A 50 μm circular aperture was used. The shot frequency was 20 Hz. A line scan was performed with a scan speed of 20 $\mu\text{m s}^{-1}$ and was c. 250 s long following a 10 s gas blank. The helium flow was fixed at 600 mL min^{-1} . The laser operations were controlled by the DigiLaz G2 software provided by CETAC. Inductively coupled plasma mass spectrometry (ICP-MS) analyses were carried out using a Bruker Aurora M90 equipped with a frequency matching RF-generator. The basic parameters were as follows: radiofrequency power 1.30 kW; plasma argon gas flow rate 16.5 L min^{-1} ; auxiliary gas flow rate 1.65 L min^{-1} ; and sheath gas flow rate 0.18 L min^{-1} . All isotopes were measured without skimmer gas. No interference corrections were applied to the selected isotopes. The analysis mode used was peak hopping with 3 points per peak. Gas blank values were subtracted. The quantification was performed with a method using direct ratios to count rates of the standard similar to those of Golitko and Terrell (2012) and Rasmussen et al. (2021) [28,29]. The NIST612 standard was run before and after batches of three samples in order to monitor the stability of the beam and to act as a standard. A relative error of ca. 10% is estimated from these measurements mostly due to mineral heterogeneity of the samples. The following isotopes were analysed for: ^{29}Si , ^{44}Ca , ^{49}Ti , ^{52}Cr , ^{55}Mn , ^{57}Fe , ^{59}Co , ^{60}Ni , ^{65}Cu , ^{75}As , ^{85}Rb , ^{88}Sr , ^{107}Ag , ^{111}Cd , ^{121}Sb , ^{197}Au , ^{205}Tl , ^{208}Pb , ^{232}Th and ^{238}U .

The maximum firing temperature was estimated according to a method developed by the CHART-group at the University of South Denmark which relies on measuring the magnetic susceptibility on a stepwise re-fired sample [30]. The susceptibility data were plotted as a function of the re-heating temperature. In order to establish the firing temperature more accurately, the square of the first derivative was plotted as a function of the re-heating temperature. The first derivative was calculated as $(S_i - S_{i-1})/\delta T$, where S_i and S_{i-1} are two consecutive susceptibility measurements and δT is the temperature difference between the heating steps. A sudden break in this curve is normally observed when the initial firing temperature has been surpassed. Under some circumstances the temperatures of two firing events can be distinguished.

3. Results and Discussion

3.1. Coloured Glazes

All the white glazes analysed non-invasively in situ showed a lead-based composition. In the XRF spectra the presence of lead (Pb) signals, typical of Della Robbia glazes, and the presence of tin (Sn) used as an opacifier, was registered [10,31,32]. On glazes with a greyish tone, higher levels of iron (Fe) and manganese (Mn) were also detected. In this case, we can assume that the addition of iron and manganese-based pigments was used to darken the mixture.

Analyses of the yellow glazes indicated that they contain principally lead (Pb) and antimony (Sb) with a consistent amount of iron (Fe) in the dark yellow. The colour of green glazed tiles is due to copper (Cu) the quantity of which increases with the colour's tone.

The colouring agent responsible for blue glazes is cobalt (Co). This was confirmed by FORS, revealing the typical signals of Co^{2+} in the spectra (Figure 3) [8,17–20,22,33–35].

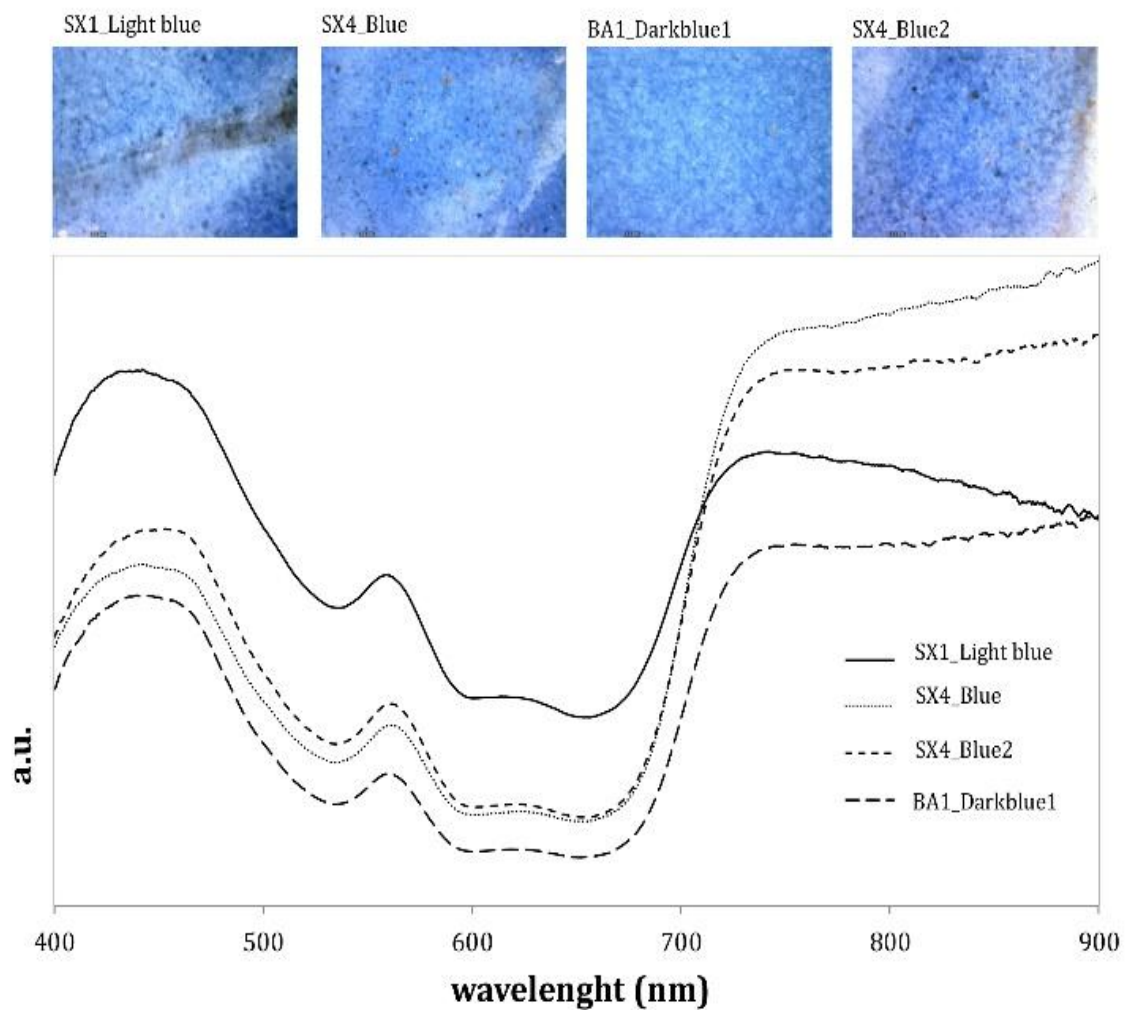


Figure 3. FORS spectra of the blue glazes analysed and the corresponding high magnification image.

As expected, the spectral features are comparable, and the percentage of reflectance is higher for the area with the lightest tone. Iron (Fe) signals are also present in all XRF spectra, highlighting the frequent combination Fe–Ni–Co reported in the literature [6,8,36]. The composition of the blue glazes, revealed by XRF, is characterized by the presence of a cobalt (Co) pigment as expected and on the absence of arsenic (As), generally associated with cobalt (Co) in most cobalt-minerals. As reported by Pappalardo 2004 [6], arsenic (As) is indeed above the detection limit in sculptures dated after 1520. Opposing this, arsenic (As) is absent in the entire production of Luca della Robbia. In order to confirm these hypotheses, a micro-sample (FED_06) was taken from a blue flower (cf. Figure 2). Microscopic examination and micro-chemical analysis revealed that this sample has a variable distribution of tin-oxide opacifying particles and the cobalt (Co) blue colourant throughout the thickness of the glaze.

The elemental composition of Della Robbia blue reported by Pappalardo [6] is in agreement with our findings. At the body-glaze interface the formation of wollastonite (CaSiO_3) is also clearly present. SEM images of the internal glaze structure and the tin oxide opacifying particles are shown in Figure 4 with the reflected light image of the cross section.

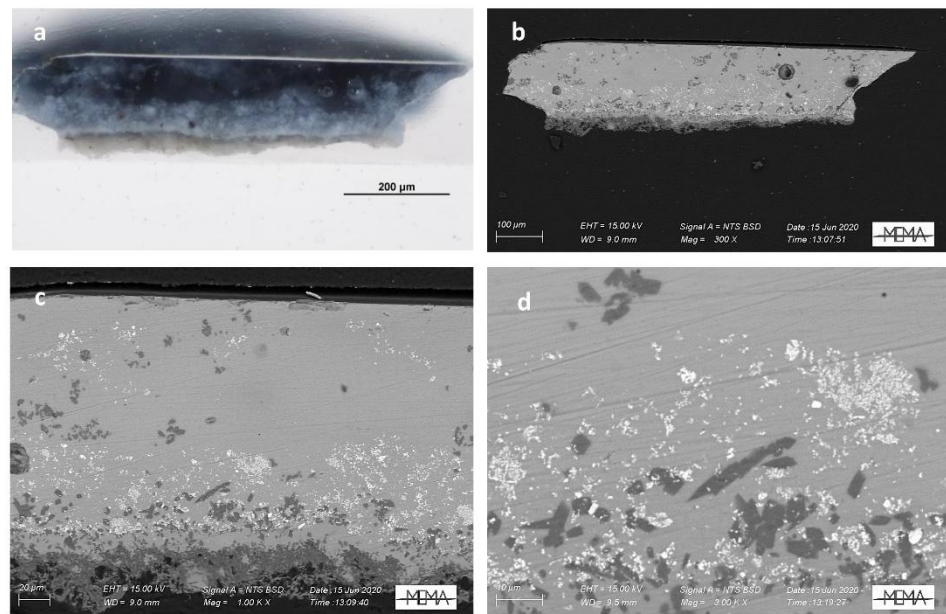


Figure 4. Visible reflected light image (a) and SEM-BSE images at different magnification (b–d) of the FED_06 sample’s cross section with details of the internal glaze structure and the tin oxide opacifying particles.

3.2. Gilding

All the tiles with traces of gilding are characterised by a yellow/orange glaze underneath. The XRF analysis highlights a comparable composition. Gold (Au) lines are evident in all the spectra of the areas analysed (except for the DX4_dor7 area) as in SX5_gold1 spectrum, shown as an example in Figure 5. It is emphasised the absence of antimony (Sb) lines ($K\alpha$ @ 26.35 KeV and $K\beta$ @ 29.72 KeV) which could have been expected linked to lead (Pb) antimoniate as a yellow colouring agent. On the contrary, in these tiles, the yellow/orange hue is linked to the colour of the terracotta underneath the glaze.

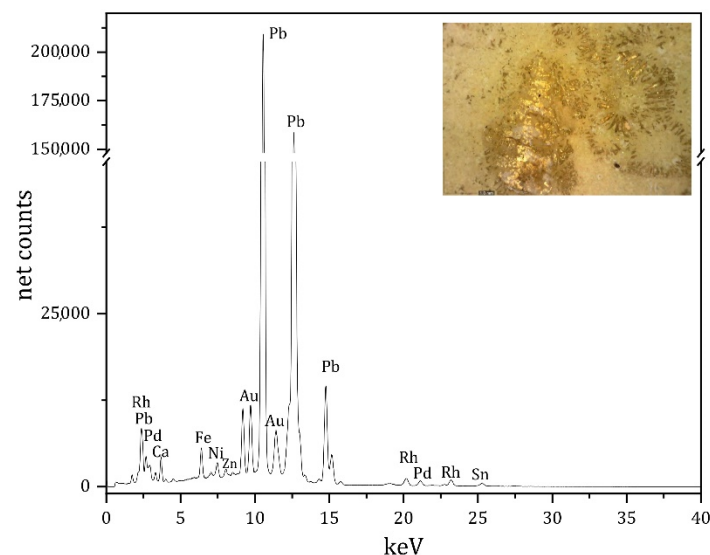


Figure 5. XRF spectrum of SX5_gold1 area. Rh and Pd are due to instrumental components, while Pb signals are “off scale” to highlight the Au lines.

The description of the gilding technique represents a challenging task. The detailed documentation of the surfaces at high magnification using the portable microscope allowed us to notice how gilding did not present itself with the homogeneity typical of cold-spread

gold leaves, as first hypothesised by the restorers. On the contrary, it appeared embedded and adhered to the level of glaze, thus appearing superficially corrugated and cracked (Figure 6).

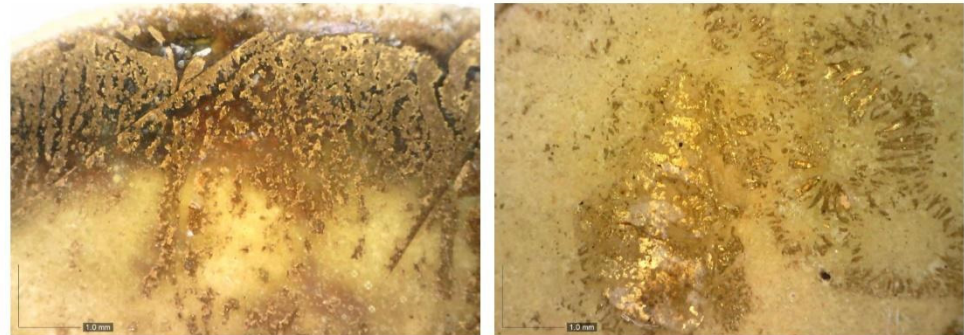


Figure 6. Details by portable microscope of three areas on gilded tiles.

The suggestion that it may be a “hot gilding” is supported by various works and texts indicating also the hypothesis of a “third firing” technique [1–4]. This last term refers to a technique where a golden foil is applied to an object or tile that has already undergone two firing phases: a preliminary firing of the terracotta support or “biscuit”; a second firing of the glaze also called “glazing”, and a third firing, done at a lower temperature than the previous ones. The gilding decorations are applied over an already melted glaze and then fired for the third time [35]. As previously stated, in order to verify the hypothesis of the use of the “third fire” technique, five micro-fragments coming from the golden tiles were analysed. The investigations carried out by the electron microscope on the cross sections, have confirmed the presence of pure gold (Au), without impurities.

Observed at high magnifications (Figure 7), the gilding appears to be executed with a golden leaf well adhered to the glaze, confirming that it is presumably applied without an organic binder. This result opens new hypotheses with respect to the previously proposed theses about the use of the “third firing” technique. However, the exact technique of making and affixing the gold leaf remains to be clarified, and further analyses must be devoted to solving this critical issue.

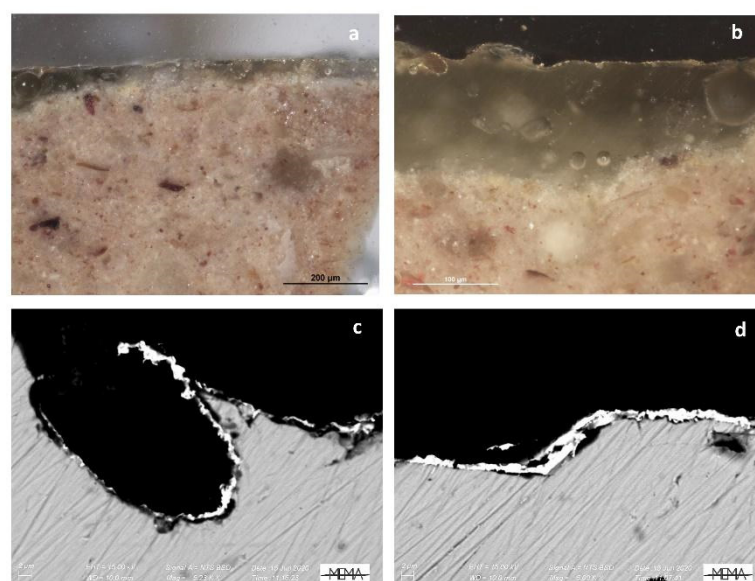


Figure 7. (a,b) Visible reflected light images of details of the cross section of sample F_02; (c,d) SEM-BSE details of the golden leaf in sample F_02.

3.3. Glazes Composition of Gilded Tiles

The thickness of the glazes ranges between 100 and 200 μm . The glassy matrix is lead-based as reported in the EDS spectrum in Figure 8.

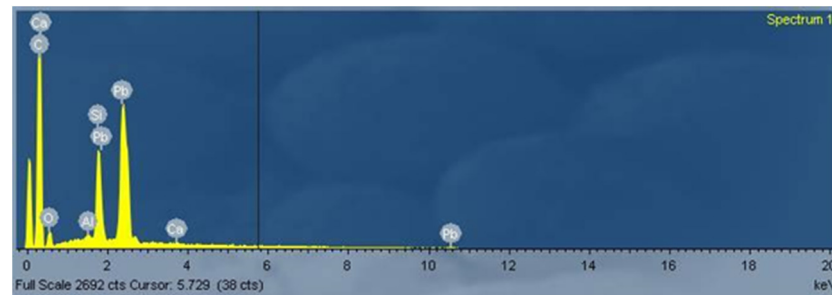


Figure 8. SEM-EDS spectrum of an area corresponding to the glaze of the sample F02.

The morphology, the chemical composition and the distribution of grains dispersed in the glassy matrix, is almost comparable from sample to sample. Few bubbles up to 40 μm in diameter and few metal–oxide complexes (such as cassiterite, SnO_2) responsible for the glaze opacity and colour, are dispersed in the matrix. In some cross-sections, tin (Sn) appears more concentrated, while in a few areas, the vitreous phase is more abundant.

At the body–glaze interface the formation of wollastonite (CaSiO_3) is clearly present in almost all samples. The interface thickness ranges between 50 up to 100 μm and its extent is related to the temperature gradient that the glaze experiences during the firing [36,37].

To the naked eye, the aspect and the colour of the sampled tiles are comparable. All the micro-fragments are sampled from gilded tiles with the peculiar, corrugated surface as previously shown (Figure 6). The analysed glazes can be grouped into three distinct types based on their structure as revealed by the SEM technique. Morphologically, the first group shows a double layer of the glaze highlighted by the images in SEM backscattered electrons (BSE) of sample F01 (Figure 9). The colour of the glaze is uniform. It is transparent over the entire surface. In the lower area in contact with the terracotta, the presence of bubbles is observed and this phenomenon, probably not intentional, confers to the glaze a greater opacity.

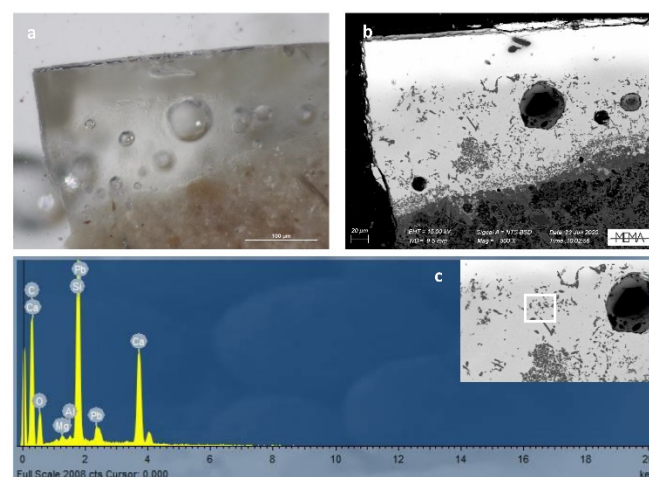


Figure 9. Visible reflected light and SEM-BSE images (a,b); detail of an area on the cross section of sample F01; (c) EDS spectrum of one of the crystals highlighted in the white box on the sample F01.

As highlighted in Figure 9, in the upper part of the glaze of sample, the characteristic needle-shaped calcium silicate crystals are totally absent. Few spare non-homogeneous bubbles are visible, suggesting the intention to obtain a transparent glaze.

In the second group of samples, the glaze exhibits calcium silicate crystals, homogeneously distributed throughout the thickness, as shown in Figure 10. The glaze looks darker with respect to the other samples. In fact, the sampled tile shows a darker hue and a more opaque and less brilliant gilding than the other tiles.

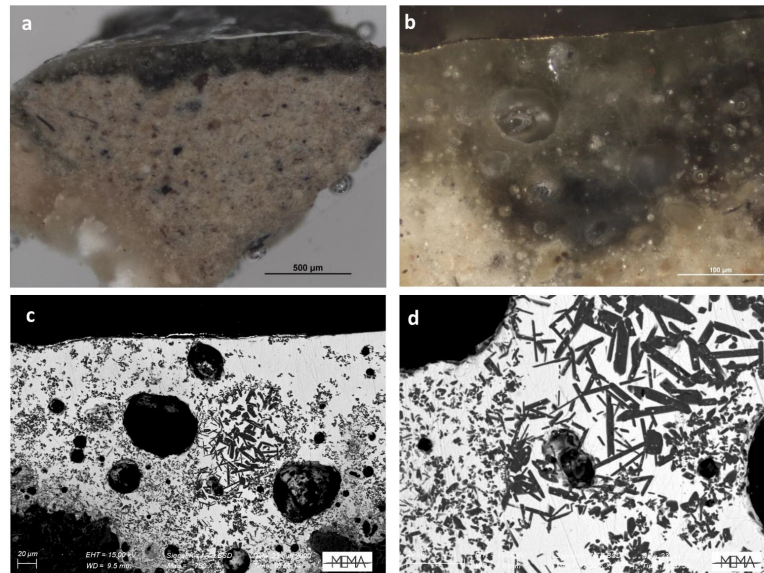


Figure 10. Visible reflected light images (a,b) and SEM-BSE image of details of sample F05fr2 (c,d), highlighting the presence of calcium silicate crystals.

The third group, on the other hand, is characterised by translucent glazes without any inclusions, except for the presence of some calcium silicate crystals present only in a thin layer in contact with the terracotta (Figure 11). The vitreous phase is transparent and characterised by the absence of bubbles.

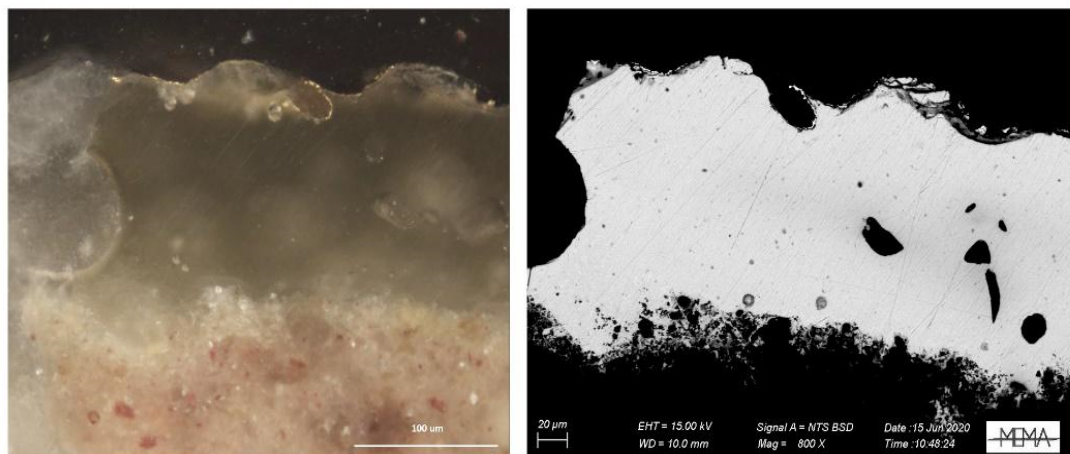


Figure 11. Visible reflected light and SEM-BSE images of sample F02.

SEM coupled with EDS has allowed a preliminary chemical analysis of various parts of the polished glaze sections. The interfaces, in general, as compared to the average glaze composition, are richer in Al, K, Ca and Si. The glaze composition for the three different groups obtained from SEM-EDS analyses is shown in Table 3.

Table 3. Mean values of oxides concentrations (wt%) measured by SEM–EDS for the groups identified on the basis of the glaze and the interface texture. We reported an average value of the composition obtained from 5 EDS areas for each glaze. The analysed area is $30 \times 30 \mu\text{m}$.

	wt% Na ₂ O	wt% MgO	wt% Al ₂ O ₃	wt% SiO ₂	wt% K ₂ O	wt% CaO	wt% PbO
F01	1.91	-	1.51	33.75	1.86	2.05	58.91
F05 fr2	-	-	1.35	38.33	-	22.56	37.82
F02	-	-	0.83	25.01	-	0.77	73.38

Observations carried out at the glaze–body interface by SEM did not allow us to determine with any doubt if the glazing mixture was applied on fired or unfired bodies. Nevertheless, as stated by Alloin et al. [36], the interaction is often increased in unfired bodies. Thus, the presence of an important interface zone may indicate the application of the glazing mixture on an unfired body. It was also demonstrated that a slower cooling or modification of the glazing mixture can generate a pronounced interface zone. In order to solve this critical issue, an evaluation on the terracotta composition has been performed.

3.4. The Terracotta Body

The ceramic mixture shows the same mineralogical and chemical characteristics in all the samples.

In Figure 12 the SEM microphotograph of a section of terracotta body is reported. A groundmass of glass-phases and relict of clay minerals are visible associated with silicate mineralogical phases.

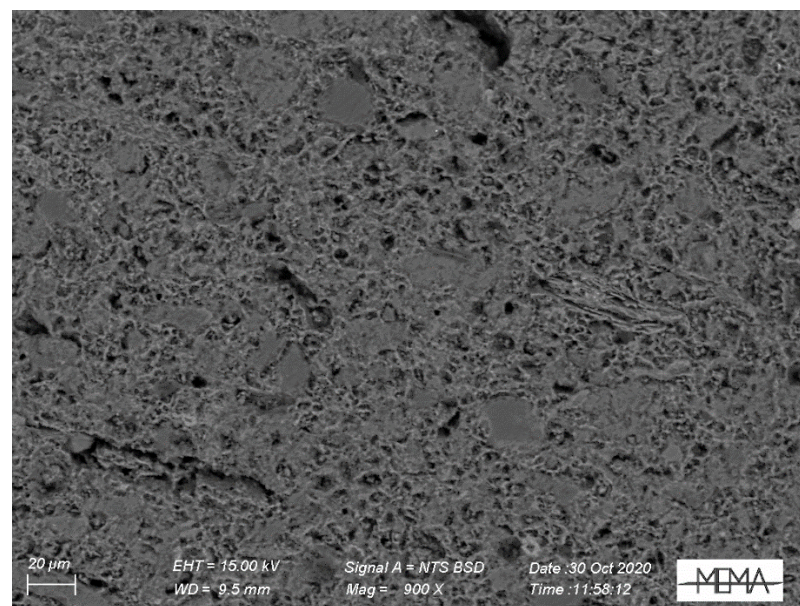


Figure 12. SEM-BSE photomicrograph of terracotta body (F_02).

From a mineralogical point of view, the XRPD analysis showed the presence of gehlenite ($\text{Ca}_2\text{Al}_2\text{SiO}_7$), wollastonite (CaSiO_3), quartz (SiO_2), calcite (CaCO_3), fassaite-diopside ($\text{CaMgSi}_2\text{O}_6$ —(Ca, Na) (Mg, Fe^{2+} , Al, Fe^{3+} , Ti) $[(\text{Si}, \text{Al})_2\text{O}_6]$) type and traces of feldspar (K feldspar— KAlSi_3O_8) and plagioclase ($\text{NaAlSi}_3\text{O}_8$ — $\text{CaAl}_2\text{Si}_2\text{O}_8$) (Figure 13). The presence of calcite (even if in small amounts) has been detected in all samples and the remarkable presence of gehlenite together with calcite. The presence of gehlenite indicates firing temperatures more than $850 \text{ }^\circ\text{C}$ [5].

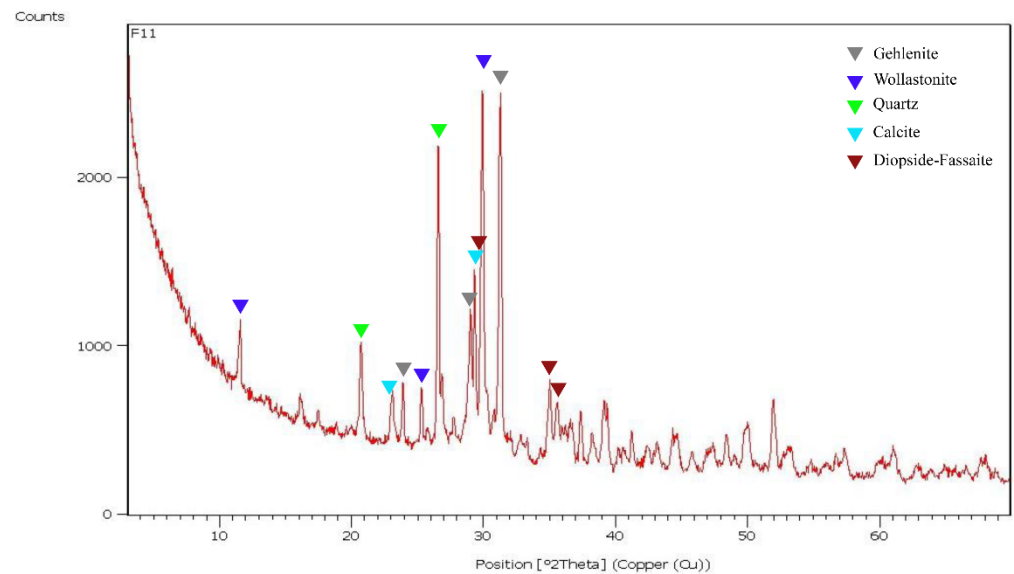


Figure 13. XRPD pattern of F11 terracotta's sample. The most intense peaks for each mineralogical phase are reported.

Major, minor and trace element concentrations for the fragments sampled to investigate the terracotta composition, have been measured by ICP-MS and are reported in Table 4.

Table 4. ICP-MS values for each element reported into weight percent oxides (wt%). Trace elements are reported in ppm of oxide. The weight percentages sum to 100.

ID	Al ₂ O ₃	SiO ₂	K ₂ O	CaO	TiO ₂	Cr ₂ O ₃	MnO	Fe ₂ O ₃	CoO	NiO	CuO	As ₂ O ₃	Rb ₂ O	SrO	Ag ₂ O	Sb ₂ O ₅	Au ₂ O	PbO	ThO ₂	U ₃ O ₈
	wt%	wt%	wt%	wt%	wt%	ppm	ppm	wt%	ppm	ppm	ppm	ppm	ppm	ppm	ppm	ppm	ppm	ppm	ppm	ppm
F11	19.0	40.3	0.859	34.9	0.797	144	1321	3.80	22.5	77.7	108	6.29	92.8	1197	1.38	0.823	0.0870	36.9	12.5	2.80
F13 a	16.9	38.6	0.862	38.8	0.794	165	1640	3.57	20.9	73.4	97.4	7.43	111	1328	0.952	1.45	0.283	1237	14.0	2.42
F13 b	16.7	38.8	0.781	38.7	0.802	166	1411	3.92	23.8	82.1	122	7.27	85.8	1710	0.869	0.970	0.252	220	16.3	2.85

The chemical and mineralogical composition gives an indication of the nature of the raw material and the technological characteristics with which the ceramic body was manufactured. The main pyrometamorphic phases found (wollastonite, gehlenite and a “ceramic pyroxene” probably fassaite-diopside type slightly Fe-, Mg- and Ca-rich) are clearly related to Ca-rich ceramic pastes [38]. The chemical analysis of the ceramic body confirms that the resource was a calcareous clay, with a lime content around 30–35 wt% CaO. There are several advantages of using calcareous clays as has been highlighted previously [39–42] and surely known very well by the craftsmen: excellent porosity in the obtained ceramic piece, strength and weather resistance and resistance to cracking after lead glaze coating [41]. Visually, the colour of the clay body is generally a light yellowish buff, even if the total iron oxide contents were in the range of 3.57–3.92 wt% Fe₂O₃. No red colour appeared, since, instead of forming hematite, the iron oxides were incorporated into calcium iron silicates [40].

In Table 5, the estimation of the firing temperature obtained by the method developed by the CHART-group at the University of South Denmark [30], which relies on measuring the magnetic susceptibility on a stepwise refired sample, is reported.

Table 5. The firing temperature estimates derived from the magnetic susceptibility and stepwise reheating.

Sample ID	T1	1 σ
	°C	°C
F11	1070	10
F13a	950	10
F13b	850	10

Both the mineralogical composition and susceptibility derived firing temperature estimates are based on the common assumption that the mineralogical assemblage has reached thermodynamic equilibrium. This may not have been the case for the samples analysed. Indeed, the co-presence of calcite and gehlenite together points to a firing event, where equilibrium was not reached. The degree to which equilibrium was not reached, and the duration of the—possibly repeated—firing events together with possible differences in cooling rates may make the estimates differ from one method to the other as well as add to the uncertainty beyond that established for equilibrium conditions.

This is probably the explanation of the two estimates of 850 and 950 °C for the two subsamples F13a and F13b, which were taken in two different depths below the surface, where the possibly unequilibrated maximum firing temperature and the cooling rates likely differed. However, overall, the different ways of estimating the firing temperature are not too different considering these caveats.

Finally, XRDP analyses on mortars and concrete (samples F_08, F_09, F_10, F_11) revealed the presence of previous restoration interventions. The main composition of mortars (F_08, F_10, F_11) is calcite, gypsum, quartz and calcium oxalate, while the sample F_09 contains also barite.

4. Conclusions

In this paper the experimental and innovative technique used by Luca della Robbia in the execution of the glazed terracotta frame was studied in depth, making new important contributions to the knowledge of the working method of the artist. The results of the investigations allowed to deepen the knowledge of the executive technique of this artwork and on the raw materials used by Luca della Robbia. Spot analyses performed by FORS and XRF made it possible to reconstruct the composition of the coloured glazes used by the artist. The chemical and mineralogical composition of the terracotta achieved by XRD, SEM-EDS and LA-ICP-MS gives an indication of the nature of the raw material and the technological characteristics with which the ceramic body was obtained. The main phases found are clearly related with Ca-rich ceramic body and the lead-based glaze is characterized by few bubbles and tin as opacifier. To understand how the gilding is carried out, it was verified that there is a possibility that the terracotta underwent several firing events. Observations carried out on samples by susceptibility derived firing temperature estimates did not allow us to determine how many firing events the bodies undergone and the applied firing temperature better than between 850 to 950 °C. The coexistence of the two phases calcite and gehlenite indicates that thermodynamic equilibrium was most likely not reached in the mineral assemblage, and this factor prevents a more precise firing temperature estimation.

Author Contributions: Conceptualization, D.M., E.C. and S.V.; methodology, D.M., E.C., S.V. and K.L.R.; formal analysis, D.M., E.C., S.V. and K.L.R.; investigation, D.M., E.C., S.V. and K.L.R.; resources, D.M., E.C., S.V. and K.L.R.; data curation, D.M., E.C., S.V. and K.L.R.; writing—original draft preparation, D.M., E.C., S.V. and K.L.R.; writing—review and editing, D.M., E.C., S.V. and K.L.R.; visualization, D.M., E.C., S.V. and K.L.R.; supervision, D.M., E.C., S.V. and K.L.R. project administration, D.M., E.C. and S.V. All authors have read and agreed to the published version of the manuscript.

Funding: This research received no external funding.

Institutional Review Board Statement: Not applicable.

Acknowledgments: Authors would like to acknowledge conservators Gabriella Tonini and Luis Pierelli from Nike Restauri for helping in the sampling and helpful discussion; Jennifer Celani to offer the permission for this research; Laura Chiarantini supporting SEM-EDS analysis. This paper is dedicated to the memory of our beloved friend and colleague Susanna Bracci who suddenly passed away during this research.

Conflicts of Interest: The authors declare no conflict of interest.

References

1. Manara, M.A.; La Tomba, J. Federighi: Un Esempio di Piccolo Fuoco nel XV Secolo? Master's Thesis, Istituto Statale d'arte per la Ceramica Gaetano Ballardini, Faenza, Italy, 1997.
2. Biavati, E. Oro metallico. decorazione a terzo fuoco sulla maiolica italiana dal Quattrocento al sec. In Proceedings of the XVIII Convegno della Ceramica, Rimini, Italy, 25–27 November 1986; pp. 11–26.
3. Severi, C. Evoluzione Delle Tecniche di Doratura in Ceramica. Master's Thesis, Istituto Statale d'arte per la ceramica Gaetano Ballardini, Faenza, Italy, 1995.
4. Deck, T. (Ed.) *Librairies-Imprimeries Réunies*; The British Museum: London, UK, 1887; pp. 270–271.
5. Amadori, M.L.; Barcelli, S.; Barcaioni, S.; Bouquillon, A.; Padeletti, G.; Pallante, P. The altarpieces of Della Robbia atelier in Marche region: Investigations on technology and provenance. *Appl. Phys. A* **2014**, *113*, 1129–1141. [[CrossRef](#)]
6. Pappalardo, G.; Costa, E.; Marchetta, C.; Pappalardo, L.; Romano, F.P.; Zucchiatti, A.; Prati, P.; Mandò, P.A.; Migliori, A.; Palombo, L.; et al. Non-destructive characterization of della Robbia sculptures at the Bargello museum in Florence by the combined use of PIXE and XRF portable systems. *J. Cult. Herit.* **2004**, *5*, 183–188. [[CrossRef](#)]
7. Zucchiatti, A.; Bouquillon, A.; Castaing, J.; Gaborit, J. Elemental analyses of a group of glazed terracotta angels from the Italian Renaissance. As a tool for the reconstruction of a complex conservation history. *Archaeometry* **2003**, *45*, 391–404. [[CrossRef](#)]
8. Zucchiatti, A.; Bouquillon, A.; Katona, I.; D'Alessandro, A. The 'della Robbia blue': A case study for the use of cobalt pigments in ceramics during the Italian Renaissance. *Archaeometry* **2006**, *48*, 131–152. [[CrossRef](#)]
9. Zucchiatti, A.; Pascual, C.; Ynsa, M.; D'Castelli, L.; Recio, P.; Criado, E.; Valle, F.J.; Climent-Font, A. Compositional analysis of XVIII century glazed. polychrome. layered porcelain by non-destructive micro α -PIXE. *J. Eur. Ceram. Soc.* **2008**, *28*, 757–762. [[CrossRef](#)]
10. Kingery, W.D.; Aronson, M. The glazes of Luca della Robbia. In *Bollettino del Museo Internazionale delle Ceramiche in Faenza LXXXVI*; Museo Internazionale delle Ceramiche: Faenza, Italy, 1990; Volume 5, pp. 221–235. ISSN 0014-679X.
11. Bouquillon, A.; Castaing, J.; Vartanian, E.; Zink, A.; Zucchiatti, A. Etude des oeuvres robbiesques au Centre de Recherche et Restauration des Musées de France. In *Les della Robbia: Sculptures en Terre Cuite Émaillée de la Renaissance Italienne*; Gaborit, J.R., Bormand, M., Eds.; Réunion des Musées Nationaux: Paris, France, 2002; pp. 139–158.
12. Bouquillon, A.; Castaing, J.; Salomon, J.; Lucarelli, F.; Mandò, P.A.; Prati, P.; Zucchiatti, A. Iba techniques to study Renaissance pottery techniques. In Proceedings of the International Conference on Fundamental & Applied Aspects of Modern Physics, Luderitz, Namibia, 13–17 November 2000; Connel, S.H., Tegen, R., Eds.; World Scientific: Singapore, 2001; pp. 441–448.
13. Bouquillon, A.; Lanterna, G.; Lucarelli, F.; Mandò, P.A.; Prati, P.; Salomon, J.; Vaccari, M.G.; Zucchiatti, A. Analisi non distruttive di smalti robbiani con fasci di ioni. In Proceedings of the Atti XXXIV Convegno Internazionale della Ceramica, Savona, Italy, 25–26 July 2001; Varaldo, C., Ed.; Edizioni del Giglio: Firenze, Italy, 2001; pp. 157–162.
14. Olson, R.J.M.; Barbour, D.S. Toward a new method for studying glazed terracottas. Examining a group of tondi by Andrea della Robbia. *Apollo* **2001**, *154*, 44–52.
15. Gentilini, G. *I Della Robbia. La scultura Invetriata nel Rinascimento*; Cantini: Florence, Italy, 1992; Volume I, p. 129.
16. Glasser, H.; Corti, G. The Litigation concerning Luca Della Robbia's Federighi Tomb. *Mitt. Kunsthistorischen Inst. Florenz* **1969**, *14*, 1–32. Available online: <http://www.jstor.org/stable/27652220> (accessed on 1 January 2022).
17. Bacci, M. Fiber optics applications to works of art. *Sens. Actuators* **1995**, *29*, 190–196. [[CrossRef](#)]
18. Bacci, M.; Picollo, M. Non-destructive spectroscopic detection of cobalt (II) in paintings and glass. *Stud. Conserv.* **1996**, *41*, 136–144.
19. Bacci, M. UV-VIS-NIR. FT-IR. FORS Spectroscopies. In *Modern Analytical Methods in Art and Archaeology*; Ciliberto, E., Spoto, G., Eds.; Chemical Analysis Series; John Wiley & Sons: New York, NY, USA, 2000; Volume 155, pp. 321–362.
20. Bacci, M.; Corallini, A.; Orlando, A.; Picollo, M.; Radicati, B. The ancient stained windows by Nicolò di Pietro Gerini in Florence. A novel diagnostic tool for non-invasive in situ diagnosis. *J. Cult. Herit.* **2007**, *8*, 235–241. [[CrossRef](#)]
21. Picollo, M.; Aceto, M.; Vitorino, T. UV-Vis spectroscopy. In *Chemical Analysis in Cultural Heritage*; Sabbatini, L., van der Werf, I.D., Eds.; De Gruyter: Berlin, Germany, 2020; pp. 253–271. ISBN 978-3-11-045641-7. [[CrossRef](#)]
22. Aceto, M.; Agostino, A.; Fenoglio, G.; Idone, A.; Gulmini, M.; Picollo, M.; Ricciardi, P.; Delaney, J. Characterisation of colourants on illuminated manuscripts by portable fibre optic UV-Visible-NIR reflectance spectrophotometry. *Anal. Methods* **2014**, *6*, 1488. [[CrossRef](#)]
23. IFAC-CNR FORS Database Fiber Optics Reflectance Spectra (FORS) of Pictorial Materials in the 270–1700 nm Range. Available online: <http://fors.ifac.cnr.it/index.php> (accessed on 1 January 2022).

24. Karidas, A.G.; Brecoulaki, H.; Bourgeois, B.; Jockey, P. In situ XRF analysis of raw pigments and traces of polychromy on marble sculpture surfaces. Possibilities and limitations. In Proceedings of the 28th International Symposium on the Conservation and Restoration of Cultural Property, “Non-destructive examination of Cultural Objects—Recent Advances in X-ray Analysis”, Tokyo, Japan, 1–3 December 2004; pp. 48–62.
25. Shugar, A.N.; Mass, J.L. *Handheld XRF for Art and Archaeology*; Leuven University Press: Leuven, Belgium, 2013.
26. Bezur, A.; Lee, L.; Loubser, M.; Trentelman, K. *Handheld XRF in Cultural Heritage*; J. Paul Getty Trust and Yale University: Los Angeles, CA, USA, 2020.
27. Pouchou, J.L.; Pichoir, F. *Quantitative Analysis of Homogeneous or Stratified Microvolumes Applying the Model “PAP”*; Heinrich, K.F.J., Newbury, D.E., Eds.; Electron Probe Quantification; Plenum Press: New York, NY, USA, 1991; pp. 31–75. [[CrossRef](#)]
28. Golitko, M.; Terrell, J.E. Mapping Prehistoric Social Fields on the Sepik coast of Papua New Guinea: Ceramic Compositional Analysis using Laser Ablation-Inductively Coupled Plasma-Mass Spectrometry. *J. Archaeol. Sci.* **2012**, *39*, 3568–3580. [[CrossRef](#)]
29. Rasmussen, K.L.; van der Plicht, J.; La Nasa, J.; Ribechini, E.; Colombini, M.P.; Delbey, T.; Skytte, L.; Schiavone, S.; Kjær, U.; Grønder-Hansen, P.; et al. Investigations of the relics and altar materials relating to the apostles St James and St Philip at the Basilica dei Santi XII Apostoli in Rome. *Herit. Sci.* **2021**, *9*, 14. [[CrossRef](#)]
30. Rasmussen, K.L.; De La Fuente, G.A.; Bond, A.D.; Mathiesen, K.K.; Vera, S.D. Pottery firing temperatures: A new method for determining the firing temperature of ceramics and burnt clay. *J. Archaeol. Sci.* **2012**, *39*, 1705–1716. [[CrossRef](#)]
31. Vaccari, M.G. *Tecniche e Materiali di Lavorazione in I Della Robbia e l’arte Nuova Della Scultura Invetriata*; Gentilini, G., Ed.; Giunti Editore: Firenze, Italy, 1998; pp. 97–116.
32. Piccolpasso, C. *The Three Books of the Potter’s Art (1557)*; Lightbown, R., Ed.; Alan Caiger-Smith Scholar Press: London, UK, 1980.
33. Barilaro, D.; Crupi, V.; Interdonato, S.; Majolino, D.; Venuti, V.; Barone, G. Characterization of blue decorated Renaissance pottery fragments from Caltagirone (Sicily, Italy). *Appl. Phys. A* **2008**, *92*, 91–96. [[CrossRef](#)]
34. Gratuze, B.; Soulier, I.; Barrandon, J.N.; Foy, D. De l’origine du cobalt dans les verres. *Rev. D’archéométrie* **1992**, *16*, 97–108. [[CrossRef](#)]
35. Ravanelli Guidotti, C. Oro e metalli preziosi per l’antica ceramica italiana. In *Ori e Tesori d’Europa. Mille Anni di Oreficeria nel Friuli Venezia Giulia (Passariano. 1992)*; Mondadori Electa: Milano, Italy, 1992; pp. 161–178. ISBN 10: 8843540777.
36. Alloin, E.; Bouquillon, A.; Gaborit, J.R. Contribution à l’étude des terres cuites glaçurées italiennes: Un tympan du milieu du XVIe siècle. *Techné* **1997**, *6*, 21–26.
37. Amara, A.B.; Schwoerer, M. Interaction between leads glazes and bodies: Research on the mode of application of the glazing mixture. In Proceedings of the 34th International Symposium on Archaeometry, Zaragoza, Spain, 3–7 May 2004; pp. 399–404.
38. Dondi, M.; Ercolani, G.; Fabbri, B.; Marsigli, M. An approach to the chemistry of pyroxenes formed during the firing of Ca-rich silicate ceramics. *Clay Min.* **1998**, *33*, 443–452. [[CrossRef](#)]
39. Tite, M.S. The production technology of Italian maiolica: A reassessment. *J. Archaeol. Sci.* **2009**, *36*, 2065–2080. [[CrossRef](#)]
40. Dias, M.I.; Prudêncio, M.I.; Kasztovszky, Z.; Maróti, B.I.; Harsányi, F.P. Nuclear techniques applied to provenance and technological studies of Renaissance majolica roundels from Portuguese museums attributed to della Robbia Italian workshop. *J. Radioanal Nucl. Chem.* **2017**, *312*, 205–219. [[CrossRef](#)]
41. Tite, M. Technological investigations of Italian Renaissance ceramics. In *Italian Renaissance Pottery*; Wilson, T., Ed.; British Museum Press: London, UK, 1991.
42. Tite, M.S.; Freestone, I.; Mason, R.; Molera, J.; Vendrell-Saz, M.; Wood, N. Lead glazes in antiquity—methods of production and reasons for use. *Archaeometry* **1998**, *40*, 241–260. [[CrossRef](#)]